Hatteras Transverse Canyon, Hatteras Outer Ridge and environs of the U.S. Atlantic margin: A view from multibeam bathymetry and backscatter

James V. Gardner *, Andrew A. Armstrong, Brian R. Calder

Center for Coastal & Ocean Mapping/NOAA Joint Hydrographic Center, University of New Hampshire, Durham, NH 03824, USA

ABSTRACT

Previously unknown features in Hatteras Transverse Canyon and environs were recently mapped during multibeam surveys of almost the entire eastern U.S. Atlantic continental margin. The newly identified features include (1) extensive landslide scarps on the walls of Hatteras Transverse and Hatteras Canyons, (2) an area of multiple landslide deposits that block lower Hatteras Transverse Canyon, (3) a large depositional feature down-canyon from the landslide deposits that rises 100 m above the uppermost Hatteras Fan and has buried the transition from the mouth of Hatteras Transverse Canyon to uppermost Hatteras Fan, (4) a zone of cyclic steps on upper Hatteras Fan that suggests supercritical turbidity currents performed a series of hydraulic jumps and formed large upstream-migrating bedforms, (5) several knickpoints in the channel thalwegs of both Hatteras Transverse Canyon and Hatteras Canyon, one 40 m high, that suggest both canyon channels are out of equilibrium and are in the process of readjusting, either to the channel blockage by the extensive landslide deposits or by a readjustments to increased sedimentation during the last eustatic lowstand, (6) a large area of outcrop on the lower margin between Pamlico and Hatteras Canyons that previously was interpreted as an area of slumps, blocky slide debris and mud waves, (7) headward erosion in the head region of Hatteras Transverse Canyon where it has intercepted the lowest reaches of Albemarle Canyon channel as well as headward erosion in a small side channel that has eroded into Hatteras Outer Ridge and (8) sections of bedforms on Hatteras Outer Ridge that are partially buried by sediment from Washington–Norfolk Canyon channel as well as by sediment transported from Hatteras Abyssal Plain. The newly discovered features add a new level of detail to understand the recent processes that have profoundly affected Hatteras Transverse Canyon, Hatteras Canyon and, to a lesser degree, Hatteras Outer Ridge.

© 2015 Elsevier B.V. All rights reserved.

1. Introduction

A submarine canyon that strikes roughly parallel, not roughly perpendicular, to isobaths on a continental margin is a very rare feature in the world ocean. In fact, transverse submarine canyons are so rare that the review of the global distribution and geomorphologies of submarine canyons by Harris and Whiteway (2011) does not mention one submarine canyon that strikes transverse to a margin. However, a few such canyons; e.g., Ameghino Transverse Canyon and Almirante Brown Transverse (sometimes referred to as the Patagonia Canyon) on the Argentine margin (Lonardi and Ewing, 1971; Hernández-Molina et al., 2009; Lastras et al., 2011) and Valencia Valley in the northwestern Mediterranean Basin (Palanques and Maldonado, 1985; Amblas et al., 2011), have been described in some detail. In all of these examples, including Hatteras Transverse Canyon on the eastern U.S. Atlantic

continental margin (Fig. 1), there is either a sediment drift (Ameghino, Almirante Brown and Hatteras Transverse Canyons) or a basement high (Valencia Channel) that has deflected sediment transport away from downslope to a cross-slope trend. The existence and uniqueness of Hatteras Transverse Canyon has been known since the late 1960s. Although, since the advent of modern commercially available multibeam echosounders (MBES) in the 1960s, Hatteras Transverse Canyon and the adjacent Hatteras Outer Ridge have not until now been mapped with a MBES. A modern deep-water MBES can map large areas of the seafloor with swaths of ~50 m/sounding spacing and even denser co-registered acoustic backscatter data that provide 3-dimensional digital views of the seafloor relief and the acoustic response of the seafloor to the MBES frequency. The area of this study (Fig. 2) was completely surveyed with a 12-kHz MBES during mapping of the bathymetry of the entire U.S. Atlantic continental margin between the 1000 and 5500 m isobaths as part of the U.S. Law of the Sea Extended Continental Shelf project (Gardner et al., 2006). The objective of this work is to use the new multibeam data to provide a three-dimensional quantitative description of the seascape at 100 m/pixel resolution, which is much higher than

* Corresponding author.
E-mail addresses: jim.ardner@unh.edu (J.V. Gardner), andya@ccom.unh.edu (A.A. Armstrong), brc@ccom.unh.edu (B.R. Calder).
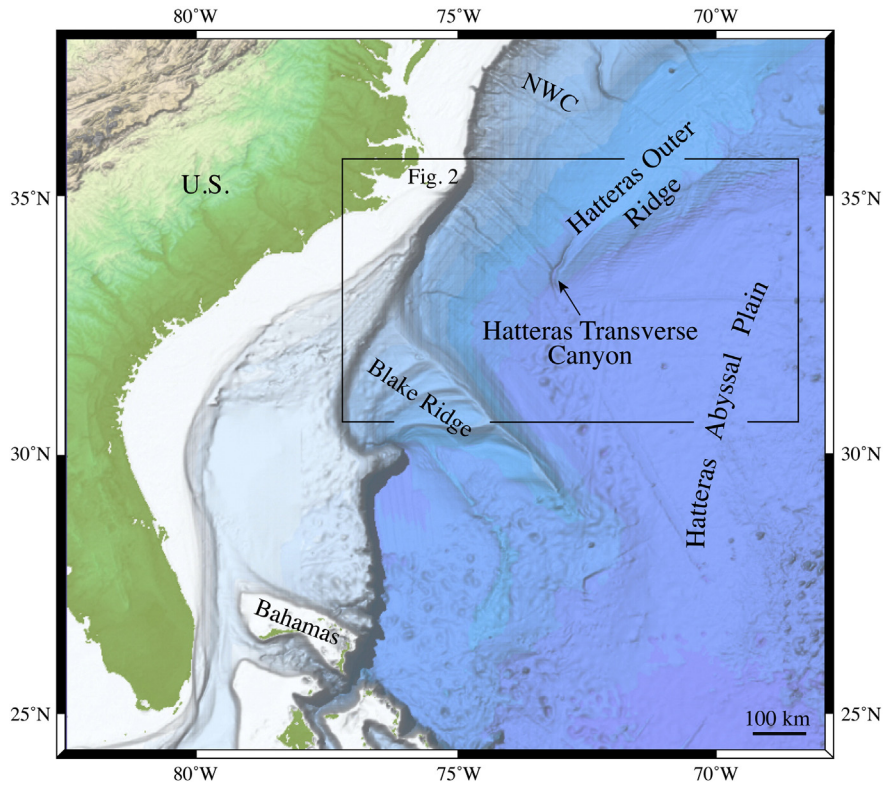
Fig. 1. Location of Hatteras Transverse Canyon, Hatteras Outer Ridge and Hatteras Abyssal Plain on the U.S. Atlantic continental margin. Bathymetry is predicted bathymetry of Smith and Sandwell (1997, v. 17.1). NWC is Norfolk–Washington Canyon. Black rectangle is the location of Fig. 2.

has been done to date for this area, and to identify various smaller-scale features that have until now not been described from this area. The digital terrain model (DTM), together with simultaneously collected co-registered acoustic backscatter, allow a better understanding of the processes that formed and modified the present seafloor than was provided by the older non-MBES data.

The traditional (pre-MBES) description of the continental margin southeast of Cape Hatteras is that of a relatively narrow 30- to 60-km-wide continental shelf, an ~95-km-wide continental slope and a broad ~375-km-wide continental rise that merges with Hatteras Abyssal Plain at approximately the 5400-m isobath. The slope and rise were constructed by deposition from turbidity currents (Drake et al., 1968; Emery et al., 1970; Pilkey and Cleary, 1986) and large mass-transport deposits (Embley and Jacobi, 1977; Embley, 1980; Twichell et al., 2009) that were subsequently modified by southward-flowing geostrophic currents that reworked the sediment (Heezen et al., 1966; McCave and Tucholke, 1986). The margin in the area of Hatteras Transverse Canyon is dominated by a series of submarine canyons and their channel extensions (here called canyon channels), especially Albemarle, Hatteras and Pamlico Canyons and to a lesser extent Washington–Norfolk Canyon (Fig. 2) and their associated canyon channels (Rona et al., 1967; Newton and Pilkey, 1969), but also by numerous smaller unnamed canyons and canyon channels. These canyons and canyon channels trend directly downslope until they are captured by Hatteras Transverse Canyon, located immediately upslope of Hatteras Outer Ridge that has served as an obstacle to continued downslope flow of turbidity currents. Hatteras Outer Ridge, a large late Tertiary to Late Pliocene sediment drift, has diverted sediments to the southwest that were initially transported directly downslope through the canyons and canyon channels to the Hatteras Abyssal Plain. The diversion of sediments formed Hatteras Transverse Canyon and redirected sediment to a more southerly location on Hatteras Fan (Cleary and Conolly, 1974). The mouth of Hatteras Transverse Canyon emerges from the southwestern end of Hatteras Outer Ridge, where

sediment has once again been diverted to the southeast by the large failure masses of Cape Fear and Cape Lookout Slides (Fig. 2) and eventually emerged onto Hatteras Fan as a series of small distributaries that spread out onto the southern Hatteras Abyssal Plain.

Work in the 1960s identified Hatteras Transverse Canyon and Hatteras Outer Ridge as somewhat anomalous features and various interpretations derived from single-beam echosounder and subbottom-profiler data were offered to explain their character. The bathymetry of Hatteras Transverse Canyon was first described by Rona et al. (1967) based on about 30 wide-angle single-beam echosounder profiles. They also produced a map of the lower reaches of Hatteras and Pamlico Canyons in the area where Hatteras Transverse Canyon captures the two canyons. They noted that the course of Hatteras Transverse Canyon roughly parallels rather than trends perpendicular to the regional isobaths, as is more typical of the other canyons and canyon channels in the region. Subsequent studies of this area using wide-angle single-beam echosounders and subbottom profilers were made by Rona and Clay (1967), Newton and Pilkey (1969), Cleary and Conolly (1974), Cleary et al. (1977), Bunn and McGregor (1980) and Pratson and Laine (1989), with seismic-reflection profiles by Tucholke and Laine (1982) and with GLORIA long-range sidescan-sonar images and widely spaced seismic profiles by Popenoe and Dillon (1996). These studies outlined the general characteristics of lower Hatteras Canyon but with widely dispersed tracklines and varying qualities of bathymetry. Rona et al. (1967) related the trend of lower Hatteras Canyon to a deflection of downslope sediment transport by Hatteras Outer Ridge. The bathymetry of Hatteras Outer Ridge was first mentioned by Heezen et al. (1959) and later investigated by Rona et al. (1967), Rona (1969), Asquith (1979), Tucholke and Laine (1982), Mountain and Tucholke (1985) and Locker and Laine (1992). Rona et al. (1967) suggested the formation of both Hatteras Transverse Canyon and Hatteras Outer Ridge, as well as bedforms on lower Hatteras Canyon (so-called "lower continental rise hills" in the descriptions from the 1960s) were due to current-controlled sedimentation related to the

Western Boundary Undercurrent that flows southwestward over the area (Heezen et al., 1966).

Prior to the development of the Hatteras Outer Ridge, a series of submarine canyons funneled sediment down the margin and out onto Hatteras Abyssal Plain. Hatteras Outer Ridge developed as some of the fine-grained sediments from gravity-driven, downslope events were intercepted by a geostrophic current presumed to be the precursor of the Western Boundary Undercurrent. A shear zone developed between the geostrophic flow and the Gulf Stream that created an area conducive to the formation of a sediment drift that eventually buried the lower reaches of the canyons and proximal submarine fans in this area (Tucholke and Laine, 1982). During the latest Pliocene, the constructional phase of Hatteras Outer Ridge was interrupted by a series of intensifications of the Western Boundary Undercurrent that were responses to the initiation of Northern Hemisphere glaciations (Tucholke and Laine, 1982). Consequently, an alternation of erosion and deposition dominated processes on Hatteras Outer Ridge throughout the Quaternary.

Prior et al. (1984) and Pratson and Laine (1989) commented that the present seascape of the entire continental margin in this area is mostly blanketed by only a few meters of Holocene sediment, suggesting to them that the large-scale geomorphology has been effectively unmodified by modern (<5 ka) processes. The only exceptions mentioned by

Prior et al. (1984) are in areas of outcrop on the middle and lower margin and in scarps on canyon walls where modern sediment has been eroded away by recent turbidity-current events.

2. Data and methods

The new MBES bathymetry and acoustic backscatter data provide complete (i.e., 100%) coverage of this area (Fig. 2) with millions of accurately located (<0.2% water depth and <5 m spatial uncertainties) soundings (depths) of variable spatial density that typically are spaced at ~50 m intervals as well as co-registered backscatter values spaced at a higher density. The sounding density allows the construction of a DTM with a maximum resolution of 100 m/pixel for the study area. The DTM was constructed from data collected on 4 cruises; two cruises in 2005 (PF05-1 and PF05-2) using a hull-mounted 12-kHz Kongsberg Maritime EM121A MBES system aboard USNS *Pathfinder*, one cruise in 2008 (KNOX17RR) with a hull-mounted 12-kHz Kongsberg Maritime EM120 MBES on RV *Roger Revelle* and a 2012 cruise (RB12-1) with the NOAA Ship *Ronald H. Brown* equipped with a hull-mounted Kongsberg Maritime 12-kHz EM122 MBES system. All three of these MBES systems have active roll, pitch and yaw beam steering. A full patch test was conducted in the survey area prior to each cruise to ensure attitude sensor offsets were correct. Sound speeds in the water column were calculated
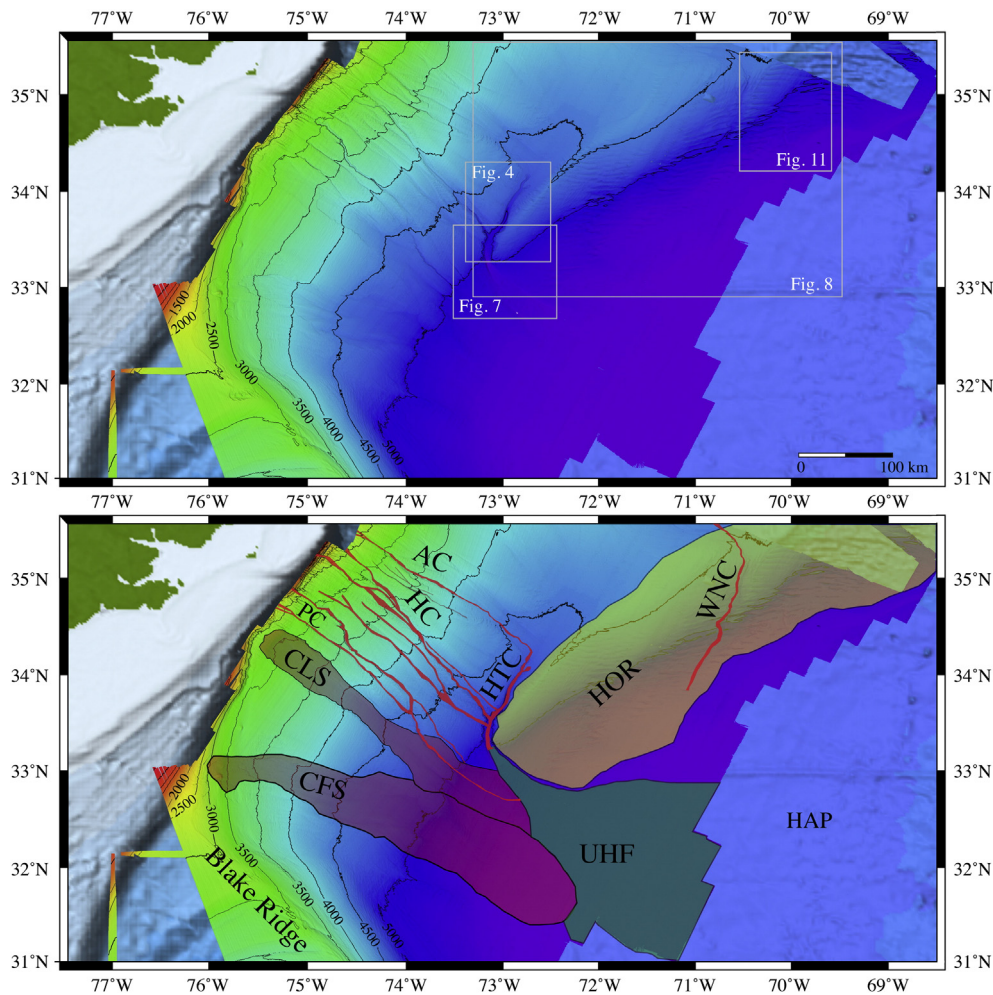
Fig. 2. A. Plan view of the MBES bathymetry (upper). White rectangles show the locations of Figs. 4, 7, 8 and 11. Annotated bathymetry (lower) with locations of Hatteras Transverse Canyon (HTC), Pamlico Canyon (PC), Hatteras Canyon (HC), Albemarle Canyon (AC), Washington–Norfolk Canyon channel (WNC), Hatteras Outer Ridge (HOR), upper Hatteras Fan (UHF), part of Hatteras Abyssal Plain (HAP), Cape Fear Slide (CFS), Cape Lookout Slide (CLS) and a section of Blake Ridge. Isobaths interval meters. B. Plan view of the MBES acoustic backscatter (upper) and the same with annotations as in panel A. White rectangle is the location of Figs. 5, 6 and 13.
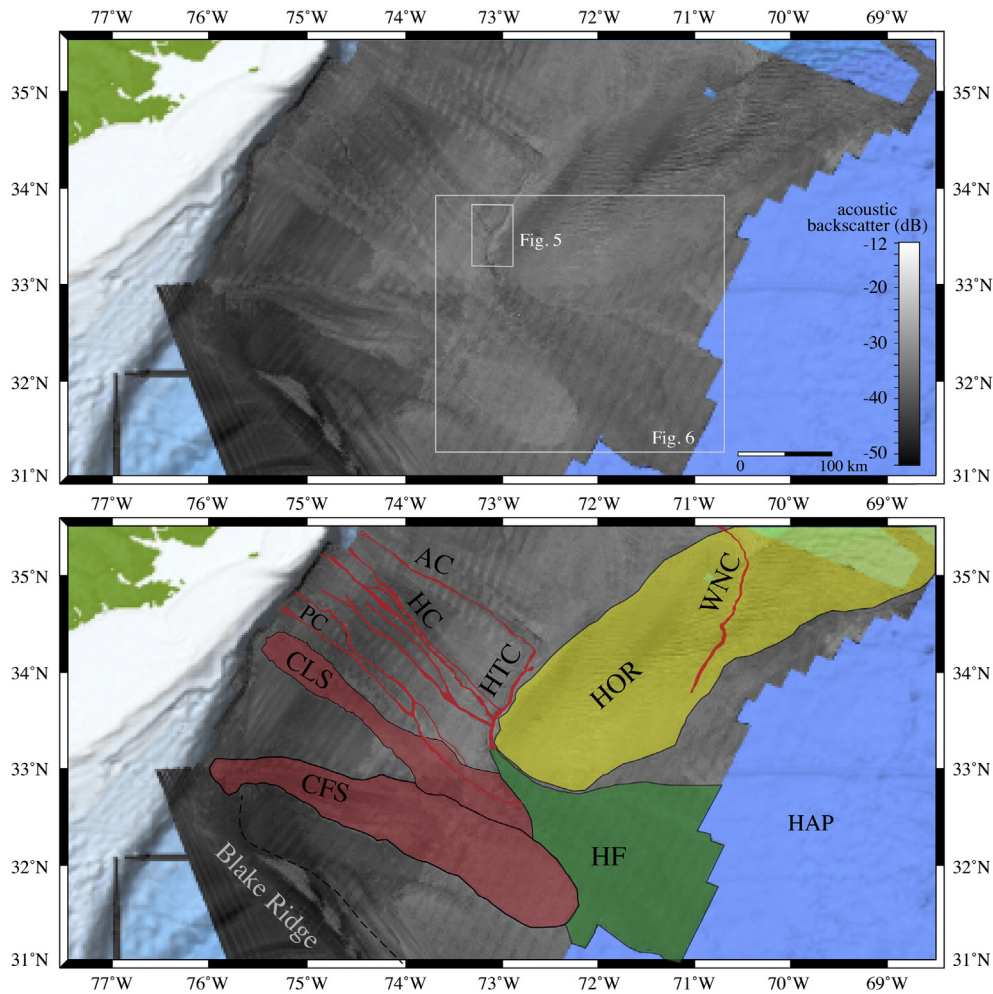
Fig. 2 (*continued*).

from calibrated multiple expendable bathythermograph casts collected at least once every 6 h on each cruise. Sound speed was integrated into the MBES data acquisition system to compensate for the refraction effects within the water column by ray tracing each sounding to its accurate location on the seafloor. Navigation on each cruise utilized an inertial motion unit (IMU) interfaced to a differential global positioning system that provided position fixes with an accuracy better than ±1 m. Data from the four cruises were combined into a single DTM with a vertical resolution of ~1 m that shows no horizontal or vertical offsets where the separate datasets join together.

The Kongsberg Maritime MBES systems collected acoustic backscatter co-registered with each bathymetric sounding. When the received amplitudes are properly calibrated to the outgoing signal strength, receiver gains, spherical spreading and attenuation, the corrected backscatter provides clues to the composition of the surficial seafloor. However, the 12-kHz acoustic signal undoubtedly penetrates the seafloor to an unknown, but perhaps significant, depth in some areas (Gardner et al., 1991), thereby generating a received backscatter value that is a function of some unknown combination of acoustic impedance, seafloor roughness and volume reverberation.

In addition to the MBES, each ship was equipped with a high-resolution Knudsen 3260 subbottom profiler. The profilers collected continuous subbottom profiles along each cruise track with a maximum penetration of ~50 m, a specified vertical resolution of 30 cm at depths greater than 1000 m and a vertical beam width of 6° to 10°.

All of the data were horizontally referenced to the WGS-84 ellipsoid and vertically referenced to instantaneous sea level.

3. Results

3.1. Hatteras Transverse Canyon System

The MBES bathymetry shows that Hatteras Transverse Canyon trends 220°, roughly parallel to the regional isobaths, with a gently curvilinear 130-km length before it exits out of its confines to form the upper portion of southern Hatteras Fan (Fig. 2). The Hatteras Transverse Canyon channel floor descends from water depths of 4718 m at its head to depths >5960 m before it is buried by landslide deposits at ~78 km down channel. The upper 38.5 km of the channel has a gradient of 0.23°, then the gradient increases to 0.32° for the next 18.3 km after which the channel abruptly steps down and the gradient flattens to 0.01° for the remaining 21.5 km before being blocked by landslide deposits. The channel width varies for the first 135 km from 0.6 to 4.4 km but then abruptly increases to between 12.3 and 43.8 km wide at ~130 km down-canyon (Fig. 3A). The channel eventually evolves into a series of distributary channels on the upper Hatteras Fan. The incision depth of Hatteras Transverse Canyon increases along the canyon length, from 60 m of relief at the head of the canyon to 325 m at 119 km down-canyon (Fig. 3B), a point just below the confluence of Hatteras Transverse Canyon with Hatteras Canyon. There are four arcuate knickpoints (i.e., abrupt steps) of the channel; a 40 m drop occurs at
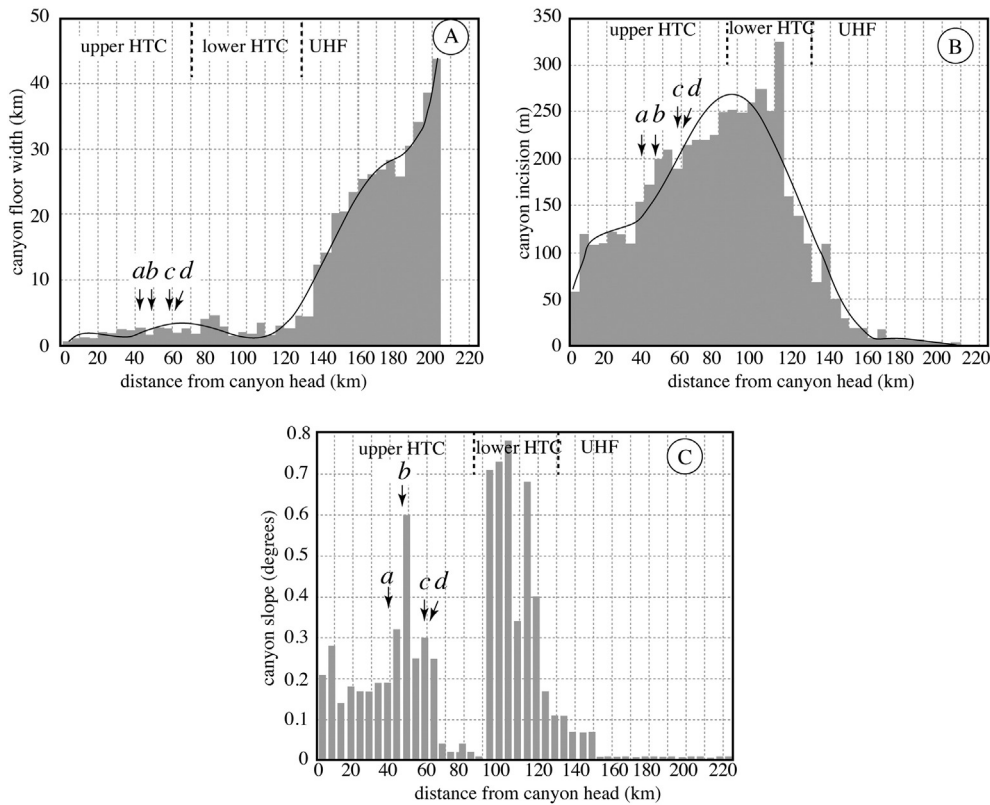
Fig. 3. Histograms of channel floor width distance down canyon (A), canyon incision depth with distance down canyon, (B), and slope of canyon floor distance down canyon (C). Lettered arrows point to knickpoints *a*, *b*, *c* and *d* in canyon channels.

41.8 km down-canyon at 4978 m water depth, a 10 m drop occurs at 48.5 km down canyon at 5015 m water depth, an 8 m drop at 58.5 km down canyon at 5073 m water depth and a 16 m drop at 61.8 km down canyon at 5081 m water depth (arrows "a" through "d", respectively, in Figs. 3C and 4). From a point 119 km down-canyon to the upper Hatteras Fan, the incision of the canyon floor decreases to below the resolution of the MBES. The upper 17 km of Hatteras Transverse Canyon has walls with slopes of 6° to 12°. The left-hand wall (when facing down-canyon) of Hatteras Transverse Canyon is generally steeper (6° to 8°) from 17 to 34.8 km down-canyon compared to the right-hand wall (2° to 4°). Up to this point (51.8 km from the head), the canyon walls show little evidence of landslide scarps. However, down-canyon beyond 51.8 km, both walls are heavily eroded with landslide scarps (Fig. 4).

The headwall of Hatteras Transverse Canyon rises almost 100 m above the canyon floor where Albermarle Canyon channel (Fig. 4) reaches the top of the Hatteras Transverse Canyon headwall. Much of the older literature called Albermarle Canyon and channel "Albermarle Transverse Canyon"; however, its trend clearly is not transverse to the isobaths except for the last 15 km (Fig. 2). The upper 5 km of Hatteras Transverse Canyon forms a loop around a central bathymetric high that stands 70 m above the eastern side of the canyon floor and 40 m above the western floor of the loop (Fig. 4). The high within the loop is 3 km by 0.9 km in plan view and is oriented N–S. The northern end of the high is aligned with the end of Albermarle Canyon channel where it enters Hatteras Transverse Canyon.

A small 8.5 km long side channel enters from the east at 16.5 km from the head of Hatteras Transverse Canyon (Fig. 4). This small side channel trends S70°W and descends 140 m with a slope of 0.7° from its head to its confluence with Hatteras Transverse Canyon channel. No step in depth occurs from the side channel floor to the main floor of Hatteras Transverse Canyon. The side channel widens towards its

head, from 0.9 km at the confluence with Hatteras Transverse Canyon to 2.4 km at its head, giving the appearance of headward erosion with 40 m of relief at the headwall. The small side channel has a maximum incision of 90 m that occurs at the confluence with Hatteras Transverse Canyon.

Landslide deposits, indicated by lumpy bathymetry elevated above the trend of the smooth channel floor, and landslide scarps occur along some, but not all, sections of Hatteras Transverse Canyon (Fig. 5). The channel floor of Hatteras Transverse Canyon, from its head to a point 54.8 km down-canyon, is very flat with relief just at or below the resolution of the 12-kHz MBES (<10 m at these depths) and the canyon walls in this section show no signs of landslide scarps. The next 23.8 km of the canyon floor continues with little relief but the canyon walls have extensive landslide scarps (Fig. 5). The series of landslide scarps on the east wall above the confluence with lower Hatteras Canyon are 21.8 km long with 300 m of relief. The opposite west wall has a series of smaller scarps with maximum relief of ~150 m. The landslides in this area have exposed at least three levels of apparent outcrops with surface dips that parallel the regional slope of the seafloor (labels 1, 2 and 3 in Fig. 4). The largest section of landslide scarps and landslide deposits on Hatteras Transverse Canyon occur 5.5 km below the confluence with lower Hatteras Canyon, 83 km from the head of Hatteras Transverse Canyon (area between black arrowheads in Fig. 5). This landslide section has extensive landslide scarps on both canyon walls, although the landslide scarps on the west wall in this section have not exposed outcrops. Landslide deposits extend for 24 km down-canyon and have accumulated as high as 25 m above the featureless channel floor that impede any present flow down-canyon. A series of large and several smaller landslide scarps are found on the channel walls that appear to be associated with the landslide deposits on the channel floor (Fig. 5). The landslide deposits were identified by constructing a series of bathymetric and acoustic backscatter profiles across both the DTM
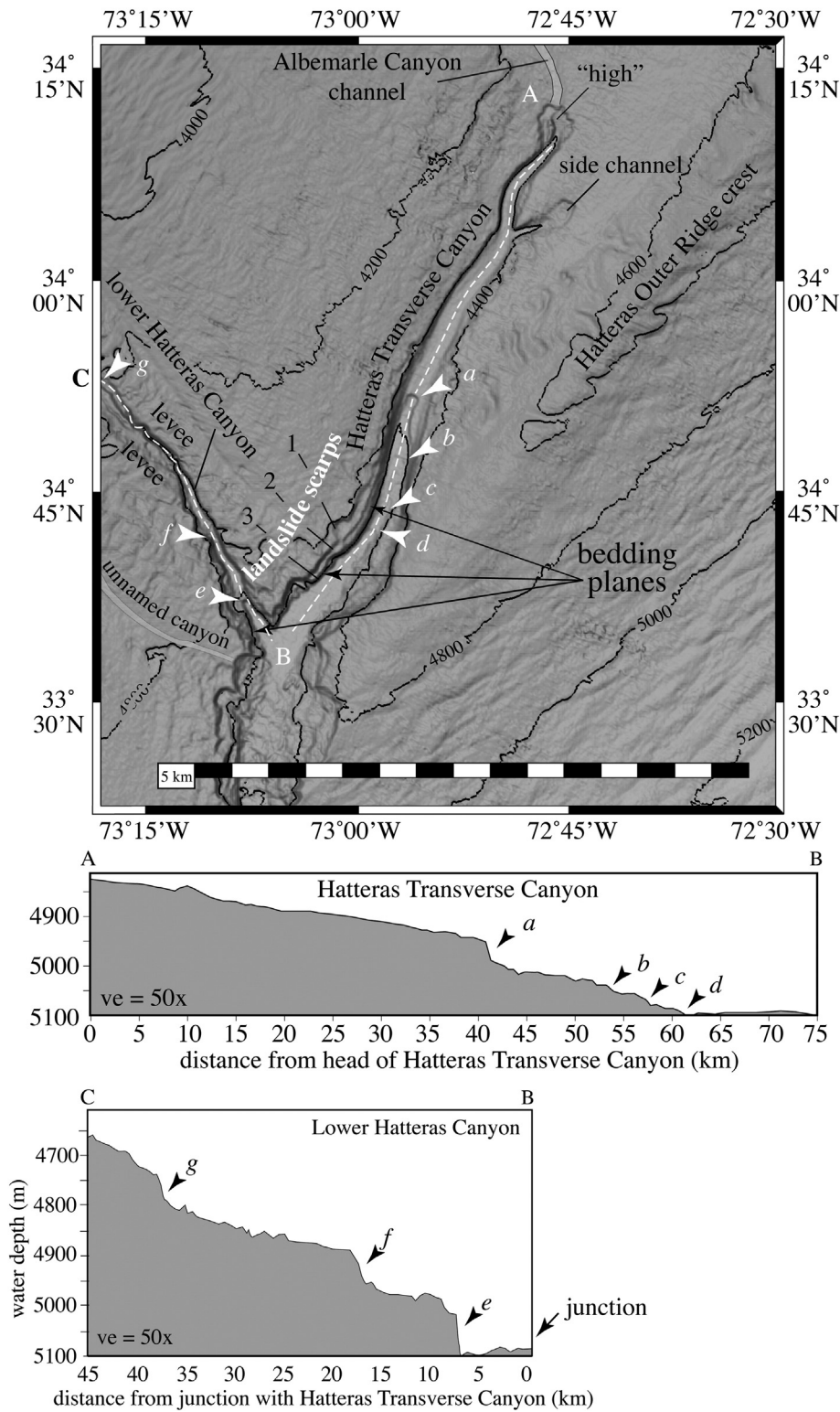
Fig. 4. Plan view of bathymetry and canyon floor profiles of Hatteras Transverse Canyon (HTC) and lower Hatteras Canyon. Location of canyon floor profile A-B-C (white capital letters) shown as white dashed line. Profiles A-B and C-B shown in lower panels. Locations of channel knickpoints *a, b, c* and *d* in Hatteras Transverse Canyon and *knickpoints e, f* and *g* in lower Hatteras Canyon are shown at white lower-case letters and arrowheads. Outcrops of bedding planes shown in black arrows and landslide scarps shown by black numbers 1, 2 and 3. Isobaths in meters. See Fig. 2A for location.

and backscatter digital mosaics that delineated individual mounds of higher relief and backscatter. The landslide deposits stand 15 to 25 m higher than the trend of the channel floor and the deposits have backscatter values that range from −28 to −26 dB that reflects a rougher microbathymetry when compared to the typically smoother adjacent

channel floor with backscatter values of −37 to −36 dB. The total volume of landslide deposits in this section of the channel is at least 20 km^3. The headwalls of the landslide scarps on the canyon walls have 50 to more than 100 m of relief with extensive debris aprons at their bases.
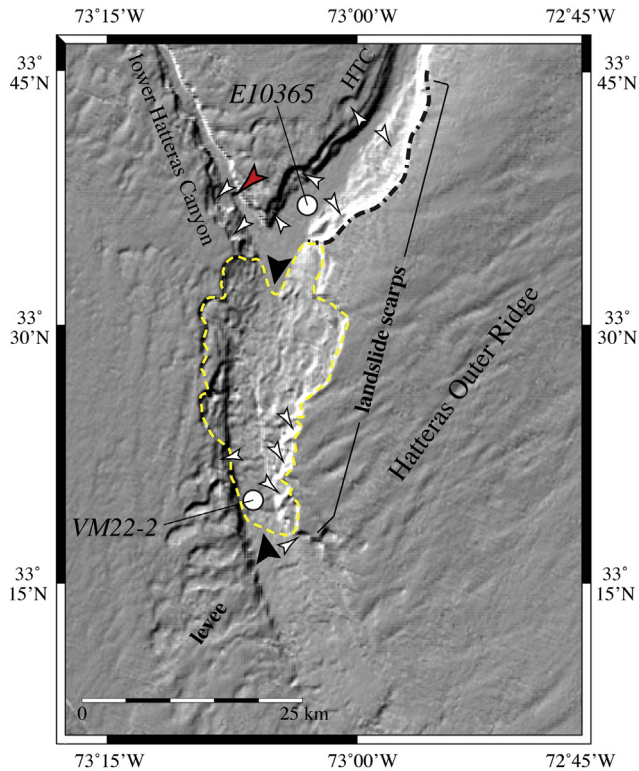
Fig. 5. Plan view of the bathymetry in the vicinity of the confluence of Hatteras Transverse Canyon (HTC) and lower Hatteras Canyon (LHC) showing extensive landslide scarps and associated landslide deposits (between black arrowheads). Outcrops on the channel walls are indicated with white arrowheads. Red arrowhead points to knickpoint *a* in lower Hatteras Canyon. White circles mark locations of piston cores VM22-2 and E10365 discussed in text. Black dashed line shows location of older landslide scarps with no indication of landslide material in the adjacent channel. Yellow dashed line shows more recent landslide scarps and associated landslide material in adjacent channel. See Fig. 2A for location. (For interpretation of the references to color in this figure legend, the reader is referred to the web version of this article.)

3.2. Lower Hatteras Canyon

Lower Hatteras Canyon trends directly downslope and enters Hatteras Transverse Canyon from the north-northwest with no step in floor depths at the confluence (Fig. 4). Compared to Hatteras Transverse Canyon, lower Hatteras Canyon is narrow with channel widths that increase from only 200 to 500 m along the lower 300 km of the canyon. An incised channel thalweg decreases in incision depth down channel from 100 to 40 m and abruptly disappears 23 km up-canyon from the confluence of lower Hatteras Canyon with Hatteras Transverse Canyon (locations e, f, and g, respectively, Fig. 4). Lower Hatteras Canyon in general has downcut from less than 100 m to as much as 260 m into the lower continental margin. The last 35 km of the channel profile of lower Hatteras Canyon has an overall gradient of 0.4° but with three knickpoints that occur at 7.5, 16 and 37.5 km up-canyon from the confluence of lower Hatteras Canyon and Hatteras Transverse Canyon. The channel floor descends 110, 70 and 60 m at the knickpoints to water depths of 5080 m, 4975 m and 4805 m, respectively (profile C–B in Fig. 4). Landslide scarps occur only on the lower 22.6 km of the canyon but there is no evidence at the resolution of the MBES data of landslide deposits on the floor of the canyon.
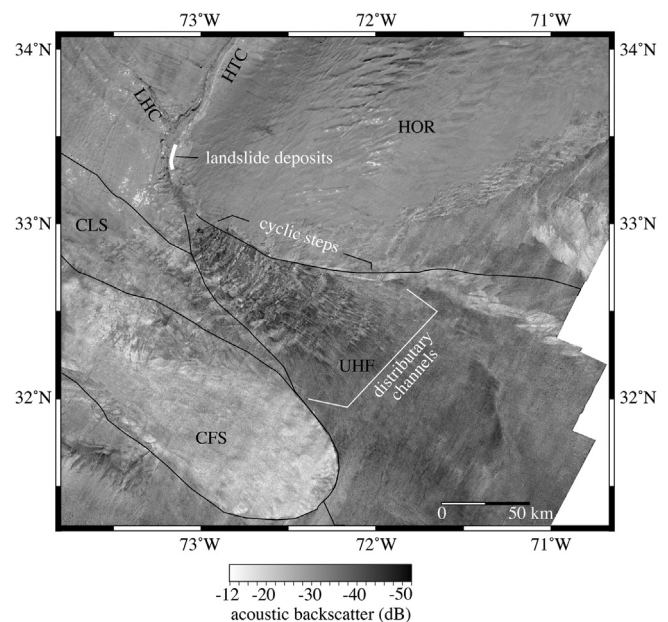
3.3. Upper Hatteras Fan

Hatteras Transverse Canyon leads directly out onto Hatteras Fan but only the upper part of Hatteras Fan was mapped with MBES. Upper Hatteras Fan (UHF) does not have a typical morphology of submarine

fans because it is confined between Hatteras Outer Ridge on the northeast and two large gravity slides, Cape Lookout (CLS) and Cape Fear Slides (CFS), on the southwest and the channel leading to the head of the upper fan is blocked by landslide deposits (Fig. 6). Levees typically on upper fans and a feeder channel that trends out onto the upper fan are not found associated with UHF. Also, a large depositional feature blocks the entire channel immediately down slope from the landslide deposits (Fig. 7). This feature is 120 km long and varies between 9 and 26 km wide with an average height above the channel floor of ~100 m that represents ~235 km³ of material. The deposit is clearly not related to the large landslide deposits found upslope as shown by the ~30 km downslope offset of the center of the deposit from the southern end of the landslide deposits and by a 70-m-deep bathymetric low between the landslide deposits and the depositional feature (Fig. 7A and B).

Upper Hatteras Fan has a zone composed of what appears to be cyclic steps (Parker, 1996; Kostic and Parker, 2006; Fildani et al., 2006; Cartigny et al., 2011; Konstic, 2011; Covault et al., 2014) that rises as much as 50 m above the main channel floor (Figs. 6 and 7) immediately downslope from the large depositional feature (Fig. 7A and C). The cyclic-step zone has 20 to 30 m of relief between successive relatively flat surfaces that are 6.5 to 13.5 km long (downslope), 1.5 to 5 km wide (edge to edge), with arcuate plan shapes that are convex downslope. The cyclic steps occur on a slope of 0.2° and abruptly die out to the southeast on a slope of 0.02°.

A series of small, very shallow curvilinear distributary (?) channels, best seen in the acoustic backscatter, can be followed for at least 73 km immediately downslope of the cyclic-step zone of the upper fan (Fig. 6). The relief of the distributary channels is below the resolution of the MBES at these depths but they are clearly defined on the acoustic backscatter image, with values of −33 dB compared to the −37 dB backscatter values of the intervening areas between the channels. The distributaries are confined to the northern edge of the upper section of the depositional feature but splay out to occupy about a third of the width of upper Hatteras Fan where the depositional feature ends and they continue to splay out downslope. These must be what Popenoe and Dillon (1996) interpreted as sediment waves from GLORIA imagery of the upper Hatteras Fan.

Fig. 6. Plan view of acoustic backscatter of upper Hatteras Fan (UHF), Cape Fear Slide (CFS), Cape Lookout Slide (CLS), the southern end of Hatteras Outer Ridge (HOR) and the lower reaches of Hatteras Transverse Canyon (HTC) and Hatteras Canyon (LHC). Location shown on Fig. 2A. Cyclic steps are described in text. Solid white line shows the extent of landslide deposits on floor of HTC. See Fig. 2B for location.
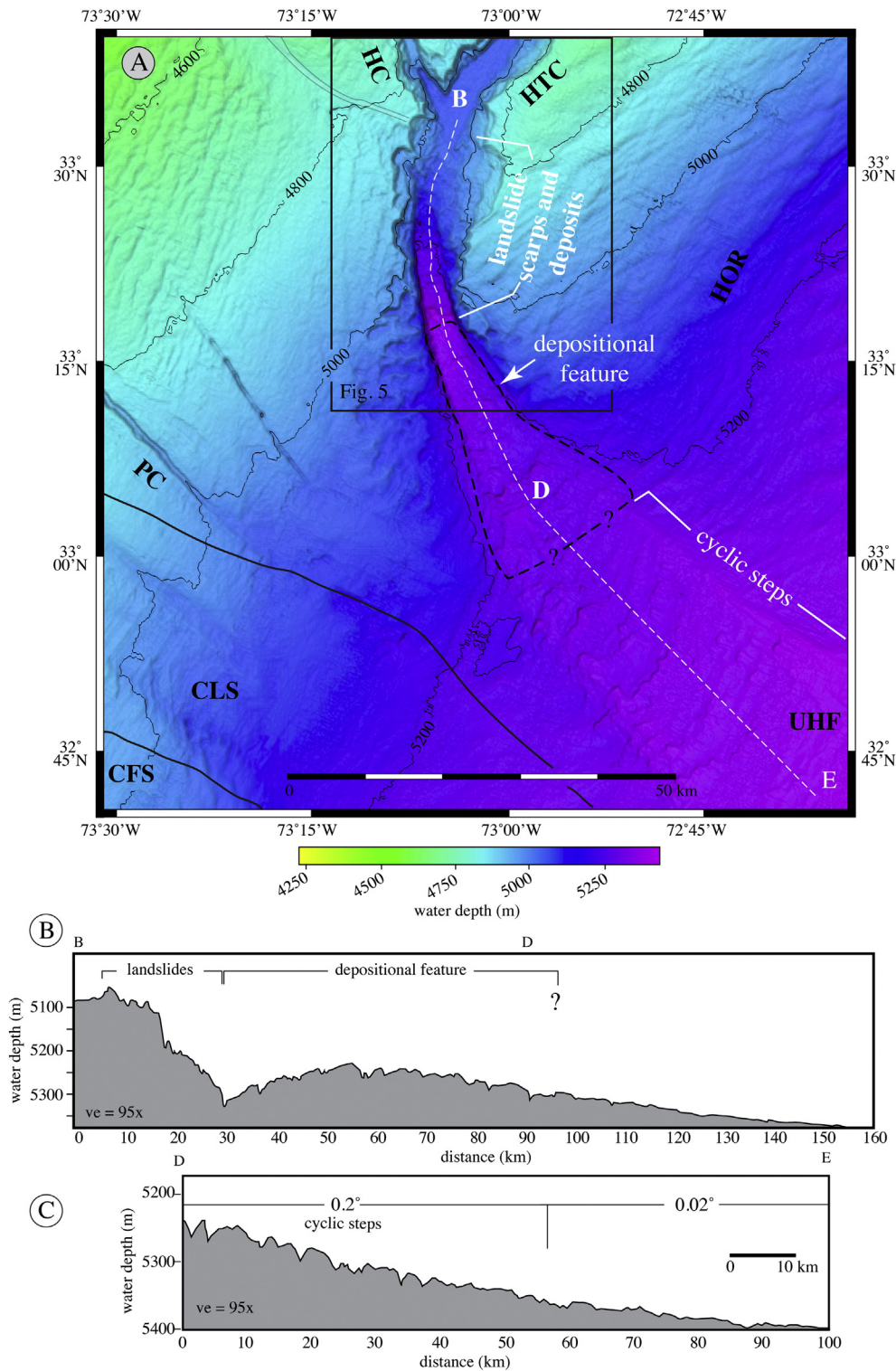
Fig. 7. (A) Plan view of bathymetry of lower-most Hatteras Transverse Canyon (HTC), upper-most Hatteras Fan (UHF) and lower-most Hatteras Canyon (HC). Landslide scarps and associated deposits occur between solid white lines. Depositional feature described in text is outlined by black dashed area. Profile B–D–E shown in dashed white line. Area of Fig. 5 shown by black rectangle. (B) Bathymetric profile B–D shows the relationship between landslide deposits that presently block transport of sediments to the depositional feature on the floor of floor of upper Hatteras Fan. (C) Subbottom profile from D to E shows cyclic steps of upper Hatteras Fan. See Fig. 2A for location.

3.4. Hatteras Outer Ridge

Only the southwestern half of Hatteras Outer Ridge was mapped with a MBES system. Hatteras Outer Ridge is a large (>19,000 km³) sediment drift immediately downslope (southeast) of Hatteras Transverse Canyon (Fig. 1) that has buried the lower reaches of Albermarle and Hatteras Canyons and the upper parts of their associated fans, as well as buried several sections of lower canyons farther to the northeast towards Hudson Canyon (Tucholke and Laine, 1982). Hatteras Outer Ridge was constructed during the Miocene to Late Pliocene (Sheridan et al., 1978; Tucholke and Laine, 1982) and is at least 700 m thick. The feature is at least 600 km long with a maximum width of ~150 km.

The crest of the southern half of Hatteras Outer Ridge trends N42°E for the first 158 km from the southwestern end, then the crest changes trend to N53°E for at least another 100 km (Fig. 8). Water depths of the crest in the southern half of the ridge range from ~4700 m at the southwest end to a minimum depth of 4360 m at a point 222 km to the northeast along the crest. The water depth of the crest slowly deepens to 4473 m northeastward at the end of the MBES data. The southern half of the ridge is asymmetrical in NW-SE cross section with slopes of 0.9° on the northwest side but with slopes of ~0.5° on the southeast side and the northwest flank is only ~10 km wide compared to as much as 140 km wide for the southeast flank because of the differences in water depths of the two flanks.

The surface of Hatteras Outer Ridge is covered with bedforms (Fig. 8) that are described in older literature as "lower continental rise hills" (Fox et al., 1968; Rona, 1969; Hollister and Ewing, 1972; Benson and Sheridan, 1978; Asquith, 1979) even though Rona (1969) correctly noted that the features are not hills but elongate ridges. The consensus by the 1980s was that these features are actually modified bedforms, not "hills" in the strict sense (Tucholke and Laine, 1982; Mountain and Tucholke, 1985), although the name "continental rise hills province" remained in later literature (e.g., Pratson and Laine, 1989; Locker and Laine, 1992). Fox et al. (1968) studied a small area of the bedforms in detail and concluded they are relict antidunes. The MBES data clearly delineate the features as bedforms and several subbottom-profiler records were collected across the bedforms during the MBES cruises that provide insights into their structure. Individual bedforms range in length from a few 10s of km to more than 200 km and their crests rise from 12 to greater than 100 m above the surface of Hatteras Outer Ridge (Fig. 9A). Wavelengths of the bedforms range from 2 to ~11 km. There is no correlation of bedform wavelength to crest water depth or bedform height (Fig. 9A–C). The bedform crests have a strong east–west orientation that is 30 to 50° off the general trend of the margin in this area (Fig. 9D). Individual bedform shapes vary from nearly symmetrical to sharply asymmetrical (Fig. 10) although there are no areas with one shape that predominates over the other. Sections of the bedform field in the middle of Hatteras Outer Ridge have been modified by channelized sediment deposition sourced from the Washington–Norfolk Canyon system (Fig. 1) that has been directed downslope and out onto the sediment drift and has partially filled in the troughs between bedforms (Fig. 11), as first noted by Rona (1969). The troughs of the bedforms in the path of this downslope transport have been filled with acoustically strong, horizontally stratified sediment (first noted by Fox et al., 1968 and shown conclusively by Hollister and Ewing (1972)). Sediment transported from the Hatteras Abyssal Plain to the east has also filled bedform troughs on the southeastern edge of Hatteras Outer Ridge (Fig. 11).

3.5. Nearby Features

3.5.1. Cape Fear Slide

Cape Fear Slide (CFS) is a major landslide that stretches more than 390 km downslope from a crown scarp at the 2411 m isobath. The
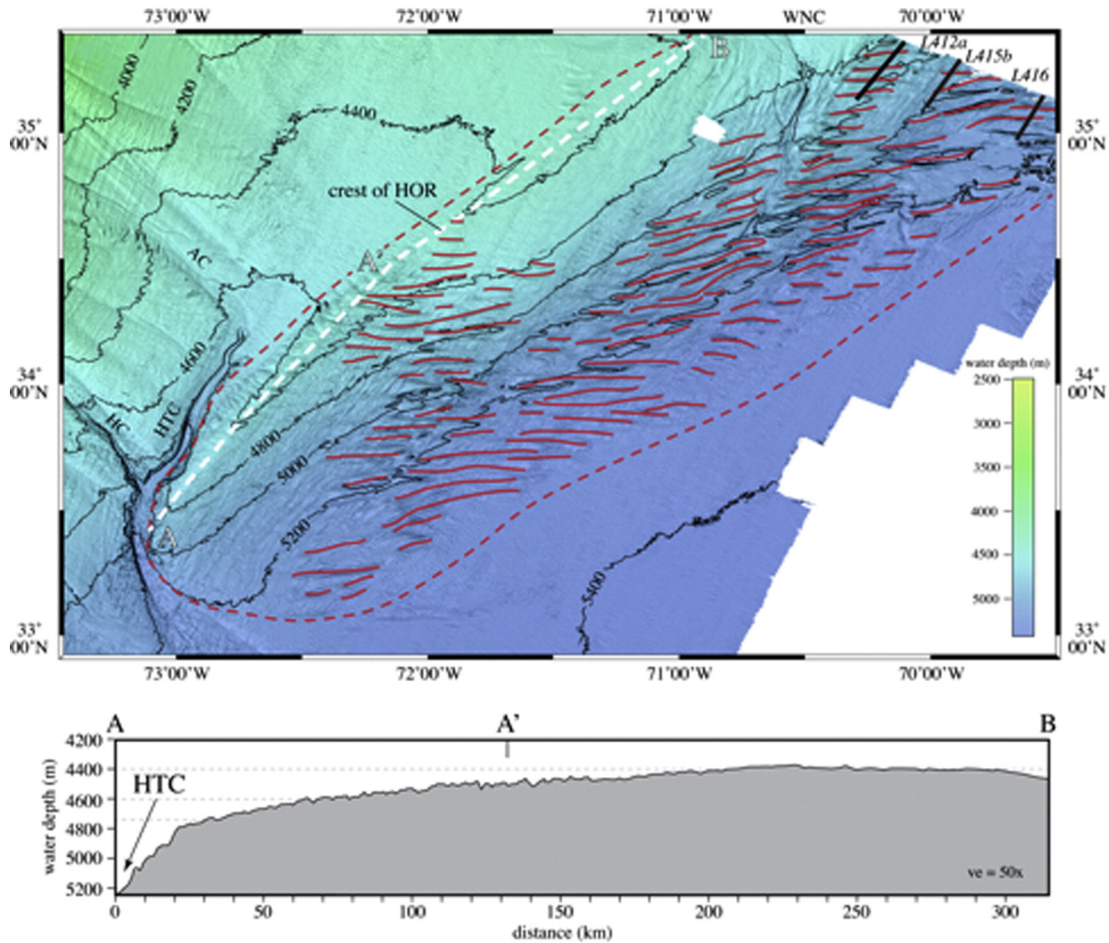
Fig. 8. Plan view of the bathymetry of Hatteras Outer Ridge (HOR) (outlined in red dashed line). Isobath interval is 200 m. White line A–A′–B is the crest of HOR and lower panel is a profile along A–A′–B. Short solid red lines are crests of bedforms. Bold white lines are locations of subbottom profiles shown in Fig. 10. HTC is Hatteras Transverse Canyon, HC is Hatteras Canyon and WNC is Washington–Norfolk Canyon channel. See Fig. 2A for location. (For interpretation of the references to color in this figure legend, the reader is referred to the web version of this article.)
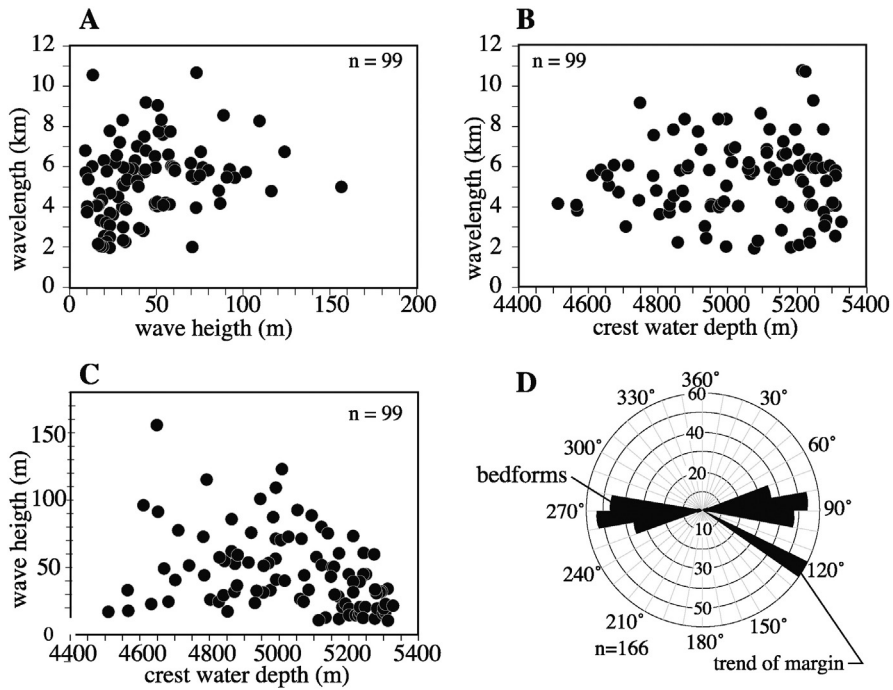
Fig. 9. (A) plot of bedform wave height vs. wavelength; (B) plot of bedform crest water depth vs. wavelength; (C) plot of bedform crest water depth vs. wave height; polar plot of bedform crest orientation compared to the trend of the regional margin in this area.

landslide was first described by Embley (1980) and later by Popenoe et al. (1993), Popenoe and Dillon (1996), Hornbach et al. (2007) and Lee (2009). The age of the Cape Fear event is 14.5 to 9 ka (Paull et al., 1996; Rodriguez and Paull, 2000). The distal toe of CFS is an abrupt 15 m wall with a slope of ~3°. The toe of the slide is 76 km wide at its widest. The northern margin of the CFS overlaps Cape Lookout Slide (discussed below) and is clear evidence that the Cape Lookout Slide occurred some time before the CFS event (Popenoe and Dillon, 1996) (Fig. 12).

3.5.2. Cape Lookout Slide

Only a section of exposed distal Cape Lookout Slide (CLS) is seen in the mapped area, located north of and partially overridden by the CFS (Fig. 12). This section of the CLS is part of a much larger slide feature that originated on the lower slope (Popenoe and Dillon, 1996). There is ~10 m of relief where the younger CFS overlaps the CLS. Although all that can be said of the age of the CLS is that it predates the CFS, the

significance of the CLS to the present study is that it forms the present western boundary of upper Hatteras Fan. The southwestern flank of upper Hatteras Fan is now buried beneath the CLS but the northeastern flank of the CLS certainly now and perhaps in the past has diverted the lower reaches of Hatteras Transverse Canyon towards the southeast and out onto the upper Hatteras Fan.

3.5.3. Area between Pamlico and Hatteras Canyons

The MBES acoustic backscatter data in the region between Pamlico and Hatteras Canyons shows a large area of anomalously high backscatter for this area (Fig. 13A and B). The anomalous area encompasses ~6500 km² and is roughly confined between the 4600 and 5150 m isobaths. Typical backscatter values outside this anomalous region range from −36 to −30 dB whereas within the anomalous area backscatter values are −28 to −25 dB. Long (~50 km), low (<15 m) linear ridges that strike N20°E, 60° to the regional slope (Fig. 13B) occur only within the high backscatter area.
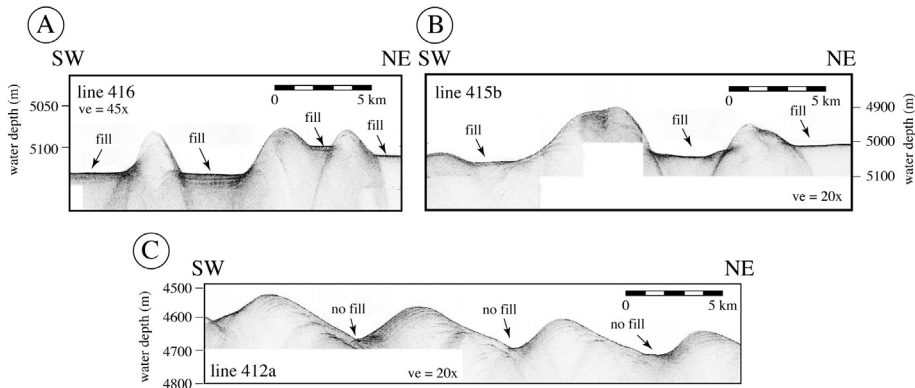
Fig. 10. (A) Symmetrical bedforms with sediment fill in troughs on subbottom line L416; (B) irregular bedforms with sediment fill in troughs on subbottom line L415b; (C) symmetrical bedforms with no fill on subbottom line L412a.
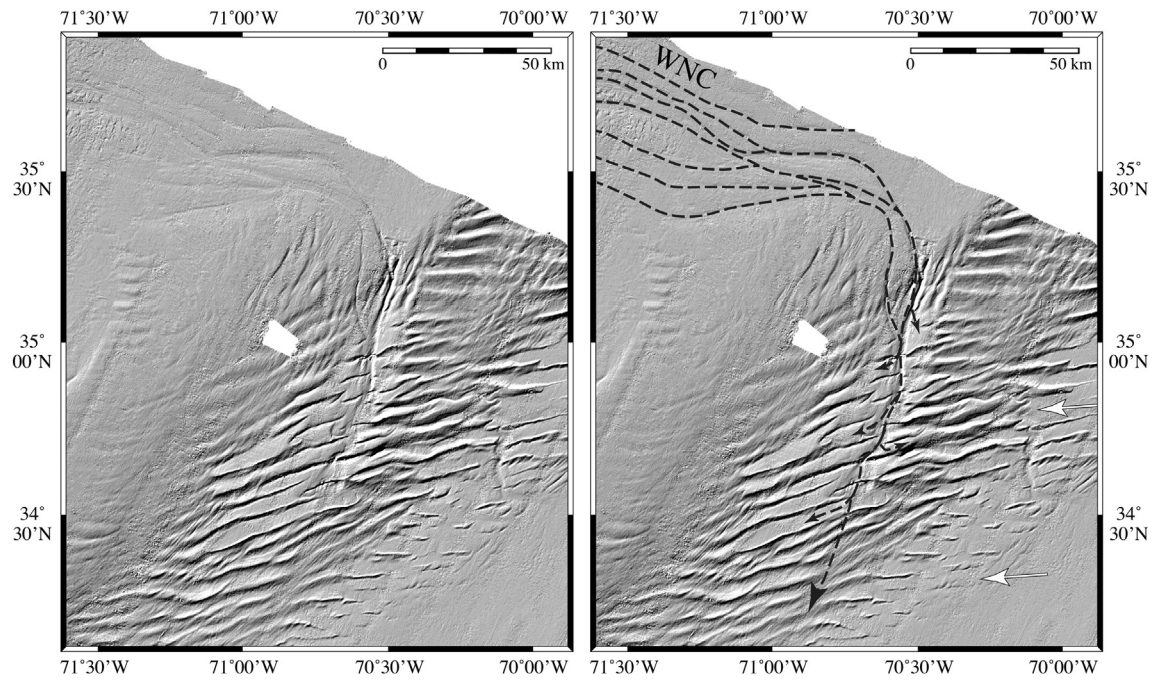
Fig. 11. (Left panel) plan view of bathymetry of central Hatteras Outer Ridge. (Right panel) same plan view as left panel showing transport paths of sediment from Washington–Norfolk Canyon-channel system (WNC) onto Hatteras Outer Ridge that has been deposited in the troughs between the bedforms. White arrows pointing west indicate direction of sediment transport from Hatteras Abyssal Plain that has partially buried bedforms. See Fig. 2A for location.

4. Discussion

Hatteras Transverse Canyon occurs in an area that includes the distal reaches of several major canyons, a large sediment drift and two large mass-failure deposits. The new multibeam bathymetry and backscatter data reveals mesoscale (i.e., ~100-m horizontal and ~5-m vertical) features that have not previously been described for this area. Newly described features include extensive landslide scarps on the walls of

Hatteras Transverse Canyon, large landslide deposits that completely block Hatteras Transverse Canyon, several knickpoints in most of the channel floors, a region of cyclic steps on upper Hatteras Fan and a large area of outcrop between Pamlico and Hatteras Canyons.

Numerous landslide scarps occur on both walls of Hatteras Transverse Canyon and the lower reaches of lower Hatteras Canyon, but for most of their length the canyon floors show no evidence of landslide deposits. The landslide deposits that were initially deposited on the
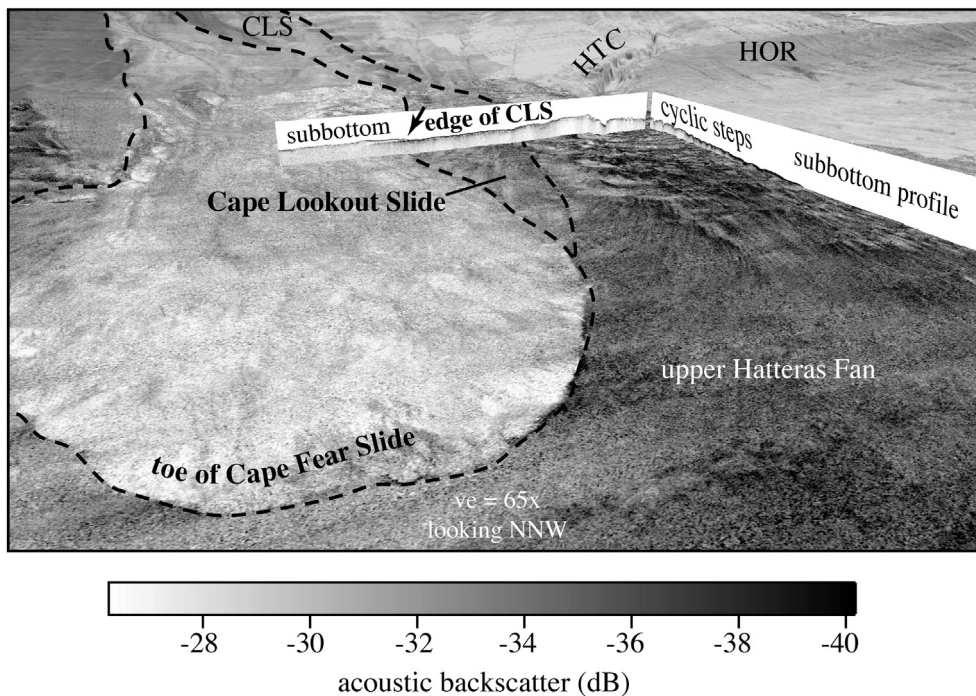
Fig. 12. Perspective view looking north-northwest of acoustic backscatter draped on bathymetry of the distal parts of Cape Fear Slide (CFS) and upper Hatteras Fan. Subbottom lines 588 and 589 show the overlap of Cape Fear Slide onto the distal Cape Lookout Slide (CLS) and the cyclic steps of the surface of the upper-most upper Hatteras Fan, respectively.
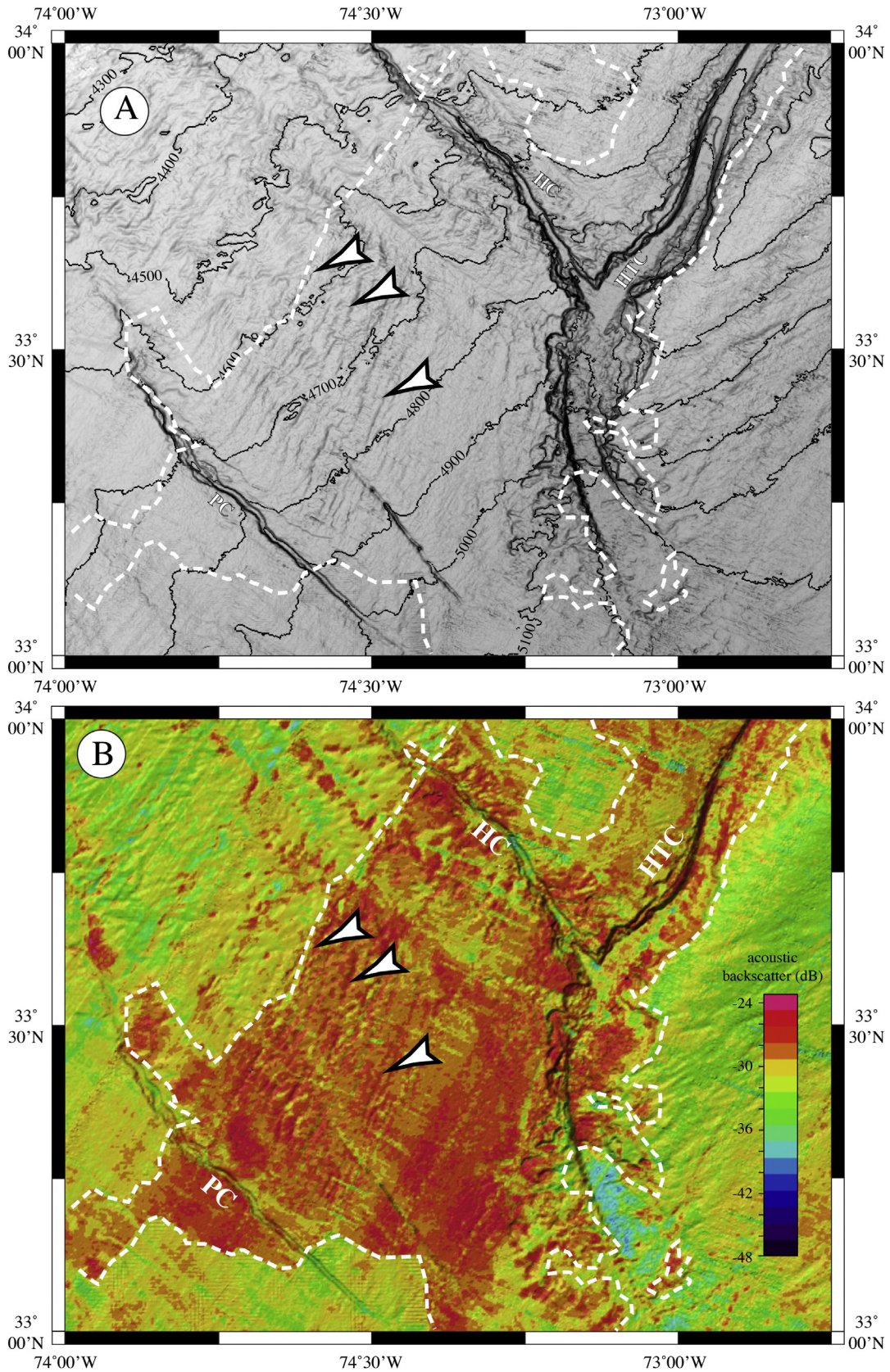
Fig. 13. Plan views of bathymetry (A) and color-coded acoustic backscatter (B) of outcrop area between Pamlico Canyon (PC) and Hatteras Canyon (HC). White dashed line encompasses outcrop area. White arrowheads point to representative linear pattern of outcrops. Isobath interval 100 m. See Fig. 2B for location.

Hatteras Transverse Canyon floor upstream of the confluence with lower Hatteras Canyon must have been reworked and transported through the lower reaches of the canyon and out onto the area below the confluence. However, immediately down canyon from the confluence of Hatteras Transverse Canyon and lower Hatteras Canyon, a large landslide complex completely blocks the lower canyon. The

composite landslide deposits are located in the immediate area of extensive landslide scarps on the wall of Hatteras Transverse Canyon below the confluence of Hatteras Transverse Canyon and lower Hatteras Canyon. The landslide deposits are 24 km long and as much as 25 m high and completely fill the channel in the landslide zone. The lack of landslide deposits on the floor of Hatteras Transverse Canyon and lower Hatteras Canyon above the confluence of Hatteras Transverse Canyon and HC suggests that the landslide scarps on the walls of Hatteras Transverse Canyon and lower Hatteras Canyon and their associated deposits are either older than the composite landslides farther down canyon or that the landslide deposits were reworked, transported down canyon and accreted to the composite landslide deposits below the confluence of Hatteras Transverse Canyon and lower Hatteras Canyon. Alternately, the landslide deposits may be older than the composite landslide deposits and make up part of the large depositional feature found farther downslope. There is no evidence on the surface of the landslide deposits that a channel has begun to incise through the deposits. This suggests that either 1) no post-landslide turbidity currents have transited through Hatteras Transverse Canyon or 2) any significant-sized post-landslide turbidity currents that flowed down Hatteras Transverse Canyon and lower Hatteras Canyon were either blocked by, or perhaps were guided over, the landslide deposits. Regardless, the distributary (?) channels on the upper Hatteras Fan are inactive channels that formed prior to the blockage by the landslide deposits. Lamont Doherty Earth Observatory piston core VM22-2 (Fig. 5) was collected from Hatteras Transverse Canyon is at the southern end of the landslide deposits. The top of the core consists of 1.72 m of medium olive gray hemipelagic sand, with a 10-cm-thick interbed of foram marl ooze that overlies a foram marl ooze. *Eastward* core 10365 (Fig. 5) was collected from Hatteras Transverse Canyon up-canyon from the landslides and is described as having a surface sand layer greater than 0.8 m thick (Field and Pilkey (1971). The lack of hemipelagic sediment at the top of the core *Eastward* 10365 suggests that Hatteras Transverse Canyon may have been an active conduit for sand transport up until the late Holocene. The surface sand layer in the *Eastward* 10365 up-canyon from the landslides, together with the surface sand layer of core VM22-2 within the landslide deposits, suggests that the landslides within Hatteras Transverse Canyon are probably Holocene in age and not Pleistocene or older, otherwise one would expect a thin hemipelagic cap on the cores. However, there is always the possibility that the surficial sediment was lost in the coring process.

It is tempting to correlate the channel knickpoints with the outcrops on the walls of Hatteras Transverse Canyon and lower Hatteras Canyon. However, the water depths of the knickpoints and outcrops do not form a plane surface or surfaces. The one exception is the channel knickpoints at 5081 m in Hatteras Transverse Canyon and at 5080 m in lower Hatteras Canyon (d and e in Fig. 5). These knickpoints may indeed be the result of excavations of resistant horizontal strata by erosion in the channels (Popenoe and Dillon, 1996). However, a more likely explanation is that all the knickpoints in the floors of Hatteras Transverse Canyon and lower Hatteras Canyon, which are all up-channel from the large landslide deposits, represent a disruption of the equilibrium profiles of both canyon channels by the landslide deposits, thus elevating the distal-most canyon channels, and that the two channels are presently headward-eroding to re-establish new equilibrium profiles. The flat, featureless nature of the channel floors of both Hatteras Transverse Canyon and lower Hatteras Canyon suggests channel entrenchment during knickpoint retreat has yet to begin (Pirmez et al., 2000; Kneller, 2003; Mitchell, 2004, 2006; Holland and Pickup, 1976; Heiniö and Davies, 2007). In addition to the knickpoints in the channel, the head of Hatteras Transverse Canyon and the side channel of upper Hatteras Transverse Canyon also appear to be eroding headward. The presence of knickpoints also could be an indication that the canyon channels are re-establishing their equilibrium profiles after a period of increased sedimentation (e.g., Amblas et al., 2011) after the last glacial lowstand, as first suggested by Embley and Jacobi (1986). Hatteras Canyon, a tributary channel to

Hatteras Transverse Canyon, must be adjusting by erosion to a drop in the thalweg of Hatteras Transverse Canyon channel, the principal channel, because there is no suggestion of a step down at the confluence of the two channel floors. Also, the channel floor of lower Hatteras Canyon is steeper (0.69°) upstream of the confluence with Hatteras Transverse Canyon than the principal channel floor (0.02°), which Mitchell (2004) suggests reflects the tributary's smaller contributing areas.

The cyclic steps described on the upper Hatteras Fan resemble in dimensions features described as cyclic steps that are thought to imply accelerated turbidity currents with supercritical turbulent flow on the stoss side and subcritical flow on the less side of the features (Parker, 1996; Kostic and Parker, 2006; Fildani et al., 2006; Cartigny et al., 2011; Konstic, 2011; Covault et al., 2014). Cyclic steps are described as predominately formed from accelerated suspended-sediment transport that generates upslope-migrating large bedforms (the steps) separated by zones of hydraulic jumps that produce erosion and sediment bypass (Konstic, 2011). These flows have been modeled from flume studies (Parker, 1996; Kostic and Parker, 2006; Cartigny et al., 2011; Konstic, 2011), as well as described offshore California in the Shepard Bend of Monterey Canyon (Fildani et al., 2006), Eel Canyon channel (Lamb et al., 2008), San Mateo Canyon (Covault et al., 2014), and Santa Monica and Redondo Canyons (Tubau et al., 2015), as well as from Horseshoe Valley in the Gulf of Cadiz (Duarte et al., 2010), Agadir Canyon off Morocco (Macdonald et al., 2011) and Setúbal Canyon off Portugal (Macdonald et al., 2011). The cyclic steps on upper Hatteras Fan may not be active today, principally because the large sediment pile may have blocked the flows upstream from the occurrence of the steps. The low channel gradients of Hatteras Transverse Canyon (0.2°) may not have accelerated turbidity current speeds fast enough to allow them to flow over the ~100-m relief of the large deposit that blocks the lower Hatteras Transverse Canyon channel. However, the 0.6° gradients of lower Hatteras Canyon may be enough to accelerate, or at least not decelerate, turbidity currents enough to run up over the large deposit. The lack of sediment cores and high-resolution subbottom profiles from these features precludes any additional speculation.

Newton and Pilkey (1969), Embley and Jacobi (1986), Pratson and Laine (1989) and Popenoe and Dillon (1996) all mention a hummocky area between Pamlico and Hatteras Canyons on the lower margin (Fig. 2A and B) as seen on seismic records and sidescan images. These authors suggested the hummocky terrain is the result of slumps, blocky slide debris or mud waves. Popenoe and Dillon (1996) concluded that the so-called hummocky area is an old landslide draped by hemipelagic sediment. This range of water depths coincides with the lower range of effects from the Western Boundary Undercurrent (Schneider et al., 1967). The high acoustic backscatter of this area (−25 to −28 vs −36 dB for the surrounding area) is also seen on the walls of Hatteras Transverse Canyon and lower Hatteras Canyon, which suggests that the high backscatter area is a region of outcrops with only a very thin sediment cover most likely because of relatively recent erosion by the Western Boundary Current.

5. Conclusions

Recent mapping the area of Hatteras Transverse Canyon and environs using high-resolution multibeam bathymetry, co-registered acoustic backscatter and 3.5-kHz subbottom profiler data allows a geomorphometric analysis of the area. The detailed digital terrain model generated from these data reveals several previously unknown important features in an area that were not identified in earlier studies. The newly discovered features add to a better understanding of the recent processes that have profoundly affected Hatteras Transverse Canyon, Hatteras Canyon and, to a lesser extent, Hatteras Outer Ridge. The newly identified features include:

- Extensive landslide scarps that are restricted to the walls of lower Hatteras Transverse Canyon and lower Hatteras Canyon.

- An area composed of a series of landslide deposits that clog Hatteras Transverse Canyon just down canyon from the confluence of Hatteras Transverse and Hatteras Canyons.
- A large depositional feature down canyon from composite landslides that may represent older landslide deposits. This deposit rises 100 m above the fan surface and appears to completely cover the transition zone between lowermost Hatteras Transverse Canyon and the uppermost Hatteras Fan.
- A series of knickpoints in the channel floor of lower Hatteras Transverse Canyon and lower Hatteras Canyon that suggest both canyon channels are in the process of reestablishing new equilibrium profiles, either because of the disruption of a former equilibrium profile by the blockage of the canyons by the extensive landslide deposits or from a period of increased sedimentation during and immediately after the last glacial eustatic lowstand.
- Headward erosion has occurred at the head region of Hatteras Transverse Canyon and has intercepted the lowest reach of Albemarle Canyon. Headward erosion has also occurred in a small side channel that has eroded into Hatteras Outer Ridge.
- Sections of the troughs between large bedforms that ornament the top of Hatteras Outer Ridge are partially buried by sediment fed from Washington–Norfolk Canyon channel as well as by sediment transported from Hatteras Abyssal Plain.
- A zone of cyclic steps occurs on the upper Hatteras Fan immediately down slope from a large depositional feature. The cyclic steps suggest vigorous supercritical turbidity currents with suspended-sediment transport flowed onto the upper fan to create the upslope-migrating cyclic-step bedforms. The age relationship between the cyclic steps and the depositional feature is unknown.
- A large (~6500 km^2) area of outcrop on the lower margin that is almost devoid of blanketing hemipelagic sediments.

Acknowledgments

References

Amblas, D., Gerber, T.P., Canals, M., Pratson, L.F., Urgeles, R., Lastras, G., Calafat, A.M., 2011. Transient erosion in the Valencia Trough turbidite systems, NW Mediterranean Basin. Geomorphology 130, 173–184.

Asquith, S.M., 1979. Nature and origin of the lower continental rise hills off the east coast of the United States. Mar. Geol. 32, 165–190.

Benson, W.E., Sheridan, R.E., 1978. Initial reports of the deep sea drilling project. Deep Sea Drilling Project 44. U.S. Government Printing Office, Washington (1005 pp.).

Bunn, A.R., McGregor, B.A., 1980. Morphology of the North Carolina continental slope, western North Atlantic, shaped by deltaic sedimentation and slumping. Mar. Geol. 37, 253–266.

Cartigny, M.J.B., Postma, G., van den Berg, J.H., Mastbergen, D.R., 2011. A comparative study of sediment waves and cyclic steps based on geometries, internal structures and numerical modeling. Mar. Geol. 280, 40–56.

Cleary, W.J., Conolly, J.R., 1974. Hatteras deep-sea fan. J. Sediment. Petrol. 44, 1140–1154.

Cleary, W.J., Pilkey, O.H., Ayers, M.W., 1977. Morphology and sediments of three ocean basin entry points, Hatteras Abyssal Plain. J. Sediment. Petrol. 47, 1157–1170.

Covault, J.A., Kostic, S., Paull, C.K., Ryan, H.F., Fildani, A., 2014. Submarine channel initiation, filling and maintenance from sea-floor geomorphology and morphodynamic modelling of cyclic steps. Sedimentology 61, 1031–1054.

Drake, C.L., Ewing, J.I., Stockard, H.P., 1968. The continental margin of the eastern United States. Can. J. Earth Sci. 5, 933–1010.

Duarte, J.C., Terrinha, P., Rosas, F.M., Valadares, V., Pinheiro, L.M., Matias, L., Magalhães, V., Roque, C., 2010. Crescent-shaped morphotectonic features in the Gulf of Cadiz (offshore SW Iberia). Mar. Geol. 271, 236–249.

Embley, R.W., 1980. The role of mass transport in the distribution and character of deep-ocean sediments with special reference to the North Atlantic. Mar. Geol. 38, 23–50.

Embley, R.W., Jacobi, R.D., 1977. Distribution and morphology of large submarine sediment slides and slumps on Atlantic continental margins. Mar. Geotechnol. 2, 205–228.

Embley, R.W., Jacobi, R.D., 1986. Mass wasting in the western North Atlantic. In: Vogt, P.R., Tucholke, B.E. (Eds.), The Western North Atlantic Region. Geology of North America, M. Geological Society of America, Boulder, CO, pp. 479–490.

Emery, K.O., Uchupi, E., Phillips, J.D., Bowin, C.O., Bunce, E.T., Knott, S.T., 1970. Continental rise of eastern North America. Am. Assoc. Pet. Geol. Bull. 54, 44–108.

Field, M.E., Pilkey, O.H., 1971. Deposition of deep-sea sands: comparison of two areas of the Carolina continental rise. J. Sediment. Petrol. 41, 526–536.

Fildani, A., Normark, W.R., Kostic, S., Parker, G., 2006. Channel formation by flow stripping: large-scale scour features along the Monterey East Channel and their relation to sediment waves. Sedimentology 53, 1265–1287.

Fox, P.J., Heezen, B.C., Harian, A.M., 1968. Abyssal anti-dunes. Nature 220, 470–472.

Gardner, J.V., Field, M.E., Lee, H., Edwards, B.E., Masson, D.G., Kenyon, N., Kidd, R.B., 1991. Ground truthing 6.5-kHz sidescan sonographs: what are we really imaging? J. Geophys. Res. 96, 5955–5974.

Gardner, J.V., Mayer, L.A., Armstrong, A., 2006. Mapping supports potential submission to U.N. Law of the Sea. EOS Trans. Am. Geophys. Union 87, 157–159.

Harris, P.T., Whiteway, T., 2011. Global distribution of large submarine canyons: geomorphic differences between active and passive continental margins. Mar. Geol. 285, 69–86.

Heezen, B.C., Tharp, M., Ewing, M., 1959. The floors of the oceans I. The North Atlantic. Geological Society of America Special Paper 65 (122 pp.).

Heezen, B.C., Hollister, C.D., Ruddiman, W.F., 1966. Shaping of the continental rise by deep geostrophic contour currents. Science 152, 502–508.

Heiniö, P., Davies, R.J., 2007. Knickpoint migration in submarine channels in response of fold growth, western Niger Delta. Mar. Pet. Geol. 24, 434–449.

Hernández-Molina, F.J., Peterlini, M., Violante, R., Marshall, P., de Isasi, M., Somoza, L., Rebesco, M., 2009. Contourite depositional system on the Argentine slope: an exceptional record of the influence of Antarctic water masses. Geology 37, 507–510.

Holland, W.N., Pickup, G., 1976. Flume study of knickpoint development in stratified sediment. Geol. Soc. Am. Bull. 87, 76–82.

Hollister, C.D., Ewing, J.I., 1972. Initial reports of the deep sea drilling project, 11. Deep Sea Drilling Project. U.S. Government Printing Office, Washington (1077 pp.).

Hornbach, M.J., Lavier, L.L., Ruppel, C.D., 2007. Triggering mechanism and tsunamogenic potential of the Cape Fear Slide complex, U.S. Atlantic margin. Geochem. Geophys. Geosyst. http://dx.doi.org/10.1029/2007GC001722 (16 pp.).

Kneller, B., 2003. The influence of flow parameters on turbidite slope channel architecture. Mar. Pet. Geol. 20, 901–910.

Konstic, S., 2011. Modeling of submarine cyclic steps: controls on their formation, migration, and architecture. Geosphere 7, 294–304.

Kostic, S., Parker, G., 2006. The response of turbidity currents to a canyon-fan transition: internal hydraulic jumps and depositional signatures. J. Hydraul. Res. 44, 631–653.

Lamb, M.P., Parsons, J.D., Mullenbach, B.L., Finlayson, D.P., Orange, D.L., Nittrouer, C.A., 2008. Evidence for superelevation, channel incision, and formation of cyclic steps by turbidity currents in Eel Canyon, California. Geol. Soc. Am. Bull. 120, 463–475.

Lastras, G., Acosta, J., Muñoz, A., Canals, M., 2011. Submarine canyon formation and evolution in the Argentine continental margin between 44°30′S and 48°S. Geomorphology 128, 116–136.

Lee, H.J., 2009. Timing of occurrence of large submarine landslides on the Atlantic Ocean margin. Mar. Geol. 264, 53–64.

Locker, S.D., Laine, E.P., 1992. Paleogene–Neogene depositional history of the middle U.S. Atlantic continental rise: mixed turbidite and contourite depositional systems. Mar. Geol. 103, 137–164.

Lonardi, A.G., Ewing, M., 1971. Sediment transport and distribution in the Argentine Basin 4. Bathymetry of the continental margin, Argentine Basin and other related provinces. Canyons and sources of sediments. In: Ahrens, L.H., Press, F., Runcorn, S.K., Urey, H.C. (Eds.), Physics and Chemistry of the Earth. Pergamon Press, New York, pp. 79–121.

Macdonald, H.A., Wynn, R.B., Huvenne, V.A.I., Peakall, J., Masson, D.G., Weaver, P.P.E., McPhail, S.D., 2011. New insights into the morphology, fill, and remarkable longevity (>0.2 m.y.) of modern deep-water erosional scours along the northeast Atlantic margin. Geosphere 7, 845–867.

McCave, I.N., Tucholke, B.E., 1986. Deep current-controlled sedimentation in the western North Atlantic. In: Vogt, P.R., Tucholke, B.E. (Eds.), The western North Atlantic Region. Geology of North America, M. Geological Society of America, Boulder, CO, pp. 451–468.

Mitchell, N.C., 2004. Form of submarine erosion from confluences in Atlantic USA continental slope canyons. Am. J. Sci. 304, 590–611.

Mitchell, N.C., 2006. Morphologies of knickpoints in submarine canyons. Geol. Soc. Am. Bull. 118, 589–605.

Mountain, G.S., Tucholke, B.E., 1985. Mesozoic and Cenozoic geology of the U.S. Atlantic continental slope and rise. In: Poag, C.W. (Ed.), Geologic Evolution of the United States Atlantic Margin. Nostrand Reinhold, New York, pp. 293–341.

Newton, J.G., Pilkey, O.H., 1969. Topography of the continental margin off the Carolinas. Southeast. Geol. 10, 87–92.

Palanques, A., Maldonado, A., 1985. Sedimentology and evolution of the Valencia Valley and fan (northwestern Mediterranean. Acta Geol. Hisp. 20, 1–19.

Parker, G., 1996. Some speculations on the relation between channel morphology and channel-scale flow structures. In: Ashworth, P.J., Bennett, S.J., Best, J.L., McLelland, S.J. (Eds.), Coherent Flow Structures in Open Channels. John Wiley & Sons Ltd., pp. 423–458.

Paull, C.K., Buelow, W.J., Ussler, W., Borowski, W.S., 1996. Increased continental-margin slumping frequency during sea-level lowstands above gas hydrate-bearing sediments. Geology 24, 143–146.

Pilkey, O.H., Cleary, W.J., 1986. Turbidity sedimentation in the northwestern Atlantic Ocean basin. In: Vogt, P.R., Tucholke, B.E. (Eds.), The Western North Atlantic region. Geology of North America, M. Geological Society of America, Boulder, CO, pp. 437–450.

Pirmez, C., Beaubouef, R.T., Friedmann, S.J., Mohrig, D.C., 2000. Equilibrium profile and base level in submarine channels: examples from late Pleistocene systems and implications for the architecture of deep-water reservoirs. In: Weimer, P., Slatt, R.M., Coleman, J.M., Rosen, N.C., Nelson, H., Bouma, A.H., Styzen, M.J., Lawrence, D.T. (Eds.), Deep-water Reservoirs of the World. Gulf Coast Section SEPM, Houston, TX, pp. 782–805.

Popenoe, P., Dillon, W.P., 1996. Characteristics of the continental slope and rise off North Carolina from GLORIA and seismic-reflection data: the interaction of downslope and contour current processes. In: Gardner, J.V., Field, M.E., Twichell, D.C. (Eds.), Geology of the United States' Seafloor: The View From GLORIA. Cambridge University Press, Cambridge, U.K., pp. 59–79.

Popenoe, P., Schmuck, E.A., Dillon, W.P., 1993. The Cape Fear landslide: slope failure associated with salt diapirism and gas hydrate decomposition. In: Schwab, W.C., Lee, H.J., Twichell, D.C. (Eds.), Submarine Landslides: Selected Studies in the U.S. Exclusive Economic Zone 2002. U.S. Geological Survey Bulletin, pp. 40–53.

Pratson, L.F., Laine, E.P., 1989. The relative importance of gravity-induced versus current-controlled sedimentation during the Quaternary along the Mideast U.S. outer continental margin revealed by 3.5 kHz echo character. Mar. Geol. 89, 87–126.

Prior, D.B., Coleman, J.M., Doyle, E.H., 1984. Antiquity of the continental slope along the middle Atlantic margin of the United States. Science 223, 926–928.

Rodriguez, N.M., Paull, C.K., 2000. ^{14}C dating of sediment of the uppermost Cape Fear slide plain: Constraints on the timing of this massive submarine landslide. In: Paull, C.K., Matsumoto, R., Wallace, P.J., Dillon, W.P. (Eds.), Proceedings of the Ocean Drilling Program. Scientific Results 164, pp. 325–327.

Rona, P.A., 1969. Linear "lower continental rise hills" off Cape Hatteras. J. Sediment. Petrol. 39, 1132–1141.

Rona, P.A., Clay, C.S., 1967. Stratigraphy and structure along a continuous seismic reflection profile from Cape Hatteras, North Carolina to the Bermuda Rise. J. Geophys. Res. 72, 2107–2130.

Rona, P.A., Schneider, E.D., Heezen, B.C., 1967. Bathymetry of the continental rise off Cape Hatteras. Deep-Sea Res. 14, 625–633.

Schneider, E.D., Fox, P.J., Hollister, C.D., Needham, H.D., Heezen, B.C., 1967. Further evidence of contour currents in the western North Atlantic. Earth Planet. Sci. Lett. 2, 351–359.

Sheridan, R.E., Enos, P., Gradstein, F., Benson, W.E., 1978. Mesozoic and Cenozoic sedimentary environments of the western North Atlantic. In: Benson, W.E., Sheridan, R.E., et al. (Eds.), Initial Reports of the Deep Sea Drilling Project 44. U.S. Government Printing Office, Washington D.C., pp. 971–979.

Smith, W.H.F., Sandwell, D.T., 1997. Global seafloor topography from satellite altimetry and ship depth soundings. Science 277, 1957–1962.

Tubau, X., Paull, C.K., Lastras, G., Caress, D.W., Canals, M., Lundsten, E., Anderson, K., Gwiazda, R., Amblas, D., 2015. Submarine canyons of Santa Monica Bay, Southern California: variability in morphology and sedimentary processes. Mar. Geol. 365, 61–79.

Tucholke, B.E., Laine, E.P., 1982. Neogene and Quaternary development of the lower continental rise off the central U.S. East Coast. In: Watkins, J.S., Drake, C.L. (Eds.), Studies in Continental Margin Geology. American Association of Petroleum Geologists Memoir 34, pp. 295–305.

Twichell, D.C., Chaytor, J.D., ten Brink, U.S., Buczkowski, B., 2009. Morphology of late Quaternary submarine landslides along the U.S. Atlantic continental margin. Mar. Geol. 264, 4–15.